Steady-State Thermal Performance Evaluation of Steel-Framed Wall Assembly with Local Foam Insulation

Jan Kosny, PhD
Member ASHRAE

Kaushik Biswas, PhD

Phillip Childs

ABSTRACT

During January and May, 2009, two configurations of steel-framed walls constructed with conventional 2 × 4 steel studs insulated with either R-19, approximately 14 cm (5.5 in.) thick, or R-13, approximately 9 cm (3.5 in.) thick, fiberglass insulation batts were tested in the Oak Ridge National Laboratory (ORNL) guarded hot box using the ASTM Standard C1363 *test procedure. The first test wall used conventional 2 × 4 steel studs insulated with 2.5 cm (1 in.) thick foam profiles, called stud-snugglers. These stud-snugglers converted the 2 × 4 wall assembly into a 2 × 6 assembly, allowing application of R-19 fiberglass insulation. The second wall tested for comparison was a conventional 2 × 4 steel stud wall using R-13 insulation batts.*

Furthermore, numerical simulations were performed in order to evaluate the steady-state thermal performance of various wood- and steel-framed wall assemblies. The effects of adding the stud-snugglers to the wood and steel studs were also investigated numerically. Different combinations of insulation and framing factor were used in the simulations.

INTRODUCTION

Wood- and steel-framed wall systems are very common in US residential and commercial buildings today. However, because metals have high thermal conductivity, the potential for thermal bridging, and consequent reduction in performance, exists in metal-framed walls. This problem is not as severe in wood-stud buildings. On the other hand, metal-framed walls have certain advantages over the wood framing, such as noncombustible construction as well as superior termite and mold resistance. Further, if suitable design modifications are made, the metal stud walls can provide thermal performance close to the wood stud walls. Kosny et al. (1997, 2002) explored methods to improve the steady-state thermal resistance of metal stud walls. These included adding exterior foam sheathing insulation, modified stud shapes, locally insulated steel studs with foam covers, etc. The authors concluded that foam-covered metal studs may perform as well as wood stud walls, while being cheaper than adding of rigid foam sheathing to conventional steel framing. It was found that the use of foam-covered studs is the simplest and an effective way of enhancing thermal performance of metal stud walls.

This article investigates the thermal effects of adding foam profiles, called stud-snugglers, in order to cover steel studs in steel framed walls. The interlocking C-shaped foam profiles are placed over the steel studs and provide local insulation between the studs and exterior structural wall sheathing. Findings of steady-state thermal performance tests of steel stud wall assemblies, with and without the addition of the foam profiles, are reported. The steel studs used in the test walls had a web thickness of 8.9 cm (3.5 in.) and a flange thickness of 3.8 cm (1.5 in.). Adding the stud-snugglers increase the web thickness, and hence the wall cavity depth, to 14 cm (5.5 in.)—equivalent to the conventional 2 × 6 wood framed wall cavity. In North America, steel stud cross-sections are usually designated according to *ASTM Standard C465-09a, Standard Specification for Nonstructural Steel Framing Members*. Due to the increased cavity depth, thicker cavity insulation layers can be applied, yielding vastly improved thermal performance. Since cavity fiber insulation is relatively

Jan Kosny *was previously a senior research scientist at the Oak Ridge National Laboratory, Oak Ridge, TN, and is currently at the Fraunhofer Center for Sustainable Energy Systems (CSE), Cambridge, MA.* ***Kaushik Biswas*** *is a post-doctoral associate and* ***Phillip Childs*** *is a staff engineer at Oak Ridge National Laboratory, Oak Ridge, TN.*

© 2010 ASHRAE.

Figure 1 *Configuration of the test steel stud wall using foam profiles and R-19 fiberglass batts.*

Figure 2 *Application of the stud-snuggler foam profile over steel stud and installation of R-19 fiberglass insulation.*

inexpensive, similar gains in thermal performance can be obtained without adding exterior foam sheathings to conventional steel frame walls of web depth 8.9 cm (3.5 in.), which can lead to substantially higher costs. These foam profiles can enable combining the desirable properties of steel studs (e.g., termite and mold resistance) with improved thermal performance. For ease of discussion and analysis, in the rest of the document, the steel studs with 14.0 cm (5.5 in.) web are referred to as 2 × 6 studs, and the steel studs with 8.9 cm (3.5 in.) web are referred as 2 × 4 studs.

Two configurations of steel-framed walls constructed with conventional 2 × 4 steel studs insulated with R-19 (approximately 14 cm [5.5 in.] thick) or R-13 (approximately 8.9 cm [3.5 in.] thick) fiberglass insulation batts were tested in the Oak Ridge National Laboratory (ORNL) guarded hot box using the procedure in *ASTM Standard C1363, Standard Test Method for Thermal Performance of Building Materials by Means of a Hot Box Apparatus*. The R-values are the nominal thermal resistances of the fiberglass batts used for testing, given in h·ft^2·°F/Btu. The equivalent thermal resistance values in SI units are 3.3 (m^2·K)/W and 2.3 (m^2·K)/W, respectively. The first test wall used conventional 2 × 4 steel studs insulated with the 1 in. thick stud-snugglers, allowing application of the R-19 fiberglass insulation in the resultant 2 × 6 assembly. The second wall tested for comparison was a conventional 2 × 4 wall using R-13 insulation batts. In addition to improving the thermal performance of metal stud walls, the addition of stud-snugglers also reduces noise transmission.

Further, a series of numerical simulations was performed to evaluate the steady-state thermal performance of various wood- and steel-frame wall assemblies. The simulations were done using Heating 7.2 (Childs 1993). The effects of adding the stud-snugglers to the wood and steel studs were also investigated numerically. Different combinations of insulation and framing factor (i.e., the percentage of the wall area occupied by the wood or steel) were used in the simulations.

DESCRIPTION OF TEST WALLS

The two walls described above were built using conventional 2 × 4 steel studs arranged 61 cm (24 in.) on center, as shown in Figure 1. In order to evaluate the effectiveness of the stud-snuggler, the wall was first tested with the steel studs in conjunction with the stud-snuggler and with 14 cm (5.5 in.) thick R-3.35 (m^2·K)/W (R-19 h·ft^2·°F/Btu) fiberglass insulation. The second test wall required disassembly of the first wall, removal of the stud-snuggler and R-19 insulation, and then reassembly using only the steel studs and approximately 9 cm (3.5 in.) thick R-2.29 (m^2·K)/W (R-13 h·ft^2·°F/Btu) insulation. Figure 2 provides a visualization of the application of snud-snugglers over 2 × 4 steel studs. This application allows the conversion of a 2 × 4 wall assembly into a 2 × 6 assembly with increased cavity thickness thereby enabling application of R-19 fiberglass insulation.

A cross-sectional view and basic dimensions of the stud-snuggler foam profile (made of extruded foam) are presented in Figure 3. The percentage of framing members in the wall was about 11%. Conventional 1.3 cm (1/2 in.) thick oriented strand board (OSB) sheathing and 1.3 cm (1/2 in.) thick gypsum boards were used in the testing.

Personnel from the ORNL Building Technologies Research Integration Center (BTRIC) constructed both test wall assemblies on site. All steel framing members were installed according to specifications provided by the manufacturer. Cavity insulation (R-19 and R-13 fiberglass batts) was custom-cut for each wall configuration to ensure the best possible fit. The exterior surfaces of the test walls were then

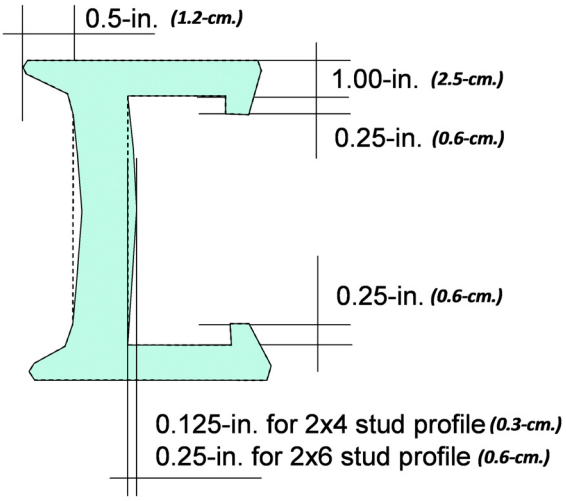

Figure 3 *Layout of one of designs of the stud-snuggler foam profile.*

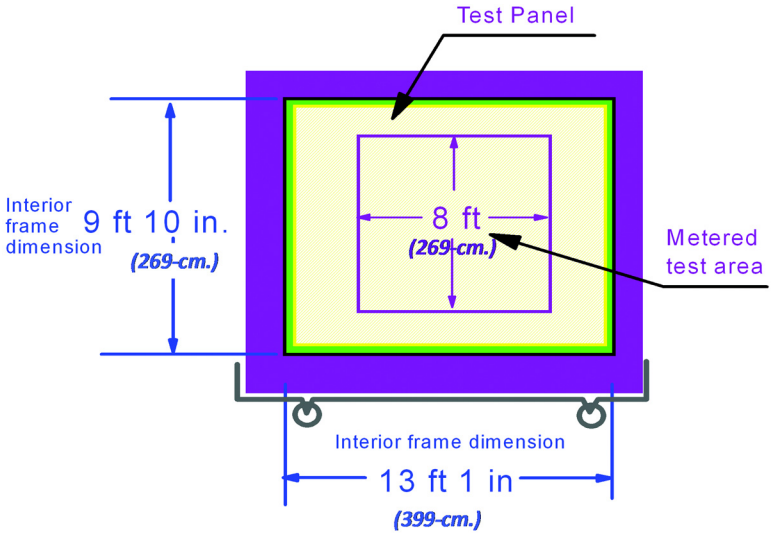

Figure 4 *Schematic of the installation of a typical wall within the hot-box test frame.*

faced with 1.3 cm (1/2 in.) thick OSB sheathing, and the interior surfaces of the test walls were faced with a 1.3 cm (1/2 in.) thick layer of gypsum board. After assembly, the completed test wall measured 2.44 m wide × 2.44 m tall (8 ft wide × 8 ft tall) and was positioned in the test frame such that the wall was centered both vertically and horizontally over the metering chamber opening. The bottom and top tracks were even with the bottom and top metering chamber gaskets. Figure 4 shows a typical installation.

The chamber conditions for this test were 37.8°C (100°F) and 10.0°C (50°F) in the metering and climate chambers, respectively. An array of thermocouples was installed on both the hot and cold sides of the test walls. The arrays for both surfaces were installed to monitor temperatures over the wall cavities, over the studs, and over the top and bottom track. The average temperatures of the hot and cold wall surfaces were determined by averaging all of the thermocouples attached to the individual components. An area-weighting method was used to determine overall external average surface temperatures.

The area of the test frame surrounding the specimen wall on both sides and the top was filled with expanded polystyrene insulation to the same thickness as the test wall. The entire perimeter of the test wall was caulked and taped to prevent air leakage.

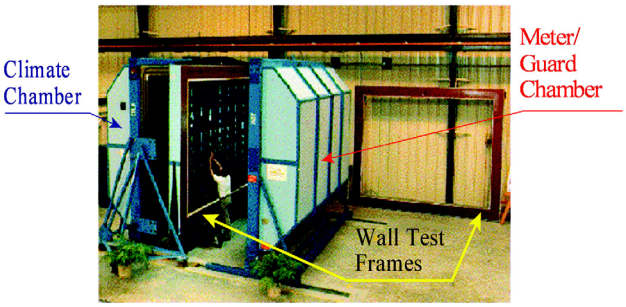

Figure 5 *Rotatable guarded hot-box used for testing.*

DESCRIPTION OF EXPERIMENTAL APPARATUS

Oak Ridge National Laboratory (ORNL) operates and maintains a guarded hot box that is used to measure the thermal resistance (R-value) and thermal transmittance (U-factor) of full-sized wall and window assemblies. The rotatable guarded hot box (RGHB) is unique in that the entire apparatus can be tilted when desired, so that appropriate test specimens can be evaluated at vertical or horizontal orientations and at any angle in between. The box operates under the requirements of *ASTM Standard C1363-97*.

Wall test assemblies were installed into a specimen frame, which was mounted on a moveable dolly. The specimen frame had an aperture of 3.96 m long × 3.05 m high (13 ft long × 10 ft high). The specimen frame/test assembly was inserted between two clam-shell chambers of identical cross sections. The placement of the test wall assembly between the chambers allowed the chamber temperatures to be independently controlled, thereby creating a temperature difference across the specimen. The chambers were designated as the climate (cold) and metering/guard (hot) chambers. A photograph of the RGHB is shown in Figure 5.

The climate chamber (cold side) was equipped with blowers and an air-conditioning system capable of producing stable environmental conditions to the extremes of –12.2°C (10°F) and 6.7 m/s (15.0 mph) wind velocity. Five centrifugal squirrel-cage air blowers, installed behind a baffle, were used to circulate the air through the airspace between the baffle and test specimen assembly. Baffle and air temperatures were measured by a series of thermocouples distributed evenly over the baffle surface. The thermocouples were distributed such that the average air and surface temperatures of the center 2.44 m × 2.44 m (8 ft × 8 ft) area facing the test specimen could also be obtained. The baffle surface facing the test specimen was painted with flat black spray paint with an emittance of 0.9.

The hot chamber consisted of two similarly shaped chambers, with the guard chamber surrounding the smaller metering chamber. The metering chamber had heaters and fans capable of producing stable environmental conditions to the extremes of 37.8°C (100°F) and 0.9 m/s (2.0 mph) wind velocity. The metering chamber was approximately 2.44 m square × 0.4 m deep (8 ft square × 1.3 ft deep) and was suspended from the inside of the guard chamber by spring loaded brackets, which constantly pushed the open face of the metering chamber up against the warm side of the test specimen. The guard chamber and the climate chamber were then sealed against each side of the test frame with separate inflatable gaskets.

All sensors inside the RGHB were connected to a data acquisition system capable of measuring either thermocouple output or raw voltage signals. Once started, the data acquisition modules automatically collected data at 30 second intervals for all sensors (except those used for measuring energy input into the metering chamber, which were on 12 second intervals). All the instrumentation and control equipment used in the RGHB are annually calibrated against National Institute of Standards and Technology (NIST) traceable standards at ORNL, or they are returned to the instrument manufacturer for calibration.

The heat flow generated by the metering chamber heaters was calculated from the voltage and current measurements taken from a precision shunt resistor as well as a watt-transducer. The energy dissipated by the metering chamber fans was metered with a precision resistor network. Once steady-state conditions were achieved, the test period continued until five successive repeated data acquisition runs (time constants [*ASTM Standard C1363-97*; Kosny and Childs 2002; Kossecka and Kosny 2008]) were obtained. The test was considered complete when each datum obtained for each measured variable differed from its mean by no more than the uncertainty of that variable. In addition, the data could not vary monotonically with time.

HOT-BOX TESTING

During January and May, 2009, two configurations of steel-framed walls were tested. One was constructed with 2 × 4 steel studs with the stud-snugglers and insulated with R-19 (14 cm [5.5 in.] thick) fiberglass insulation. The second test wall had 2 × 4 steel studs and R-13 (9 cm [3.5 in.] thick) fiberglass batts. In both walls 2 × 4 steel studs were installed either at 0.61 m (24 in.) on center. The test data were compiled and analyzed following the requirements of *ASTM Standard C1363-97*.

To calculate the meter-side and climate-side average surface temperatures, the appropriate average temperatures were combined in an area-weighted manner. The test wall surface area used for thermal measurements was 5.9 m^2 (64 ft^2). To area-weight the surface temperatures, the percentage of the total wall surface area that each individual wall component comprised was determined. For all tested walls, the average temperatures were computed by area-weighting the average cavity, stud, and track surface temperatures.

The metering box energy exchange Q_{mb} was calculated by Equation 1:

$$Q_{mb} = \frac{A_{mb} \cdot \Delta T_{mb}}{R_{mb}} \quad (1)$$

where

Q_{mb} = heat flow rate through metering box walls, W (Btu/h)
A_{mb} = surface area of metering box, m^2 (ft^2)
T_{mb} = temperature imbalance across metering box walls, °C (°F)
R_{mb} = thermal resistance of the metering box walls, $(m^2 \cdot K)/W$ $(h \cdot ft^2 \cdot °F/Btu)$

The total energy flow through the wall assembly Q_{wall} was calculated from

$$Q_{wall} = Q_h + Q_{fan} - Q_{mb} \quad (2)$$

where

Q_{wall} = total energy flow rate through the wall assembly from metering to climate chamber, W (Btu/h)
Q_h = power input to the resistance heaters in metering chamber, W (Btu/h)
Q_{fan} = power input to fans in metering chamber, W (Btu/h)

The surface-to-surface thermal resistance of the wall assembly R_{wall} is calculated from

$$R_{wall} = \frac{A_{wall} \cdot (T_{ms} - T_{cs})}{Q_{wall}} \quad (3)$$

where

R_{wall} = surface-to-surface thermal resistance of the wall assembly, $(m^2 \cdot K)/W$ $(h \cdot ft^2 \cdot °F/Btu)$
A_{wall} = area of wall, m^2 (ft^2)
T_{ms} = average metering-side surface temperature, °C (°F)
T_{cs} = average climate-side surface temperature, °C (°F)

The meter-side and climate-side air-film coefficients R_{ms} and R_{cs} are calculated by Equations 6 and 7, respectively.

$$R_{ms\ air} = \frac{A_{wall} \cdot (T_{ma} - T_{ms})}{Q_{wall}} \quad (4)$$

$$R_{cs\ air} = \frac{A_{wall} \cdot (T_{cs} - T_{ca})}{Q_{wall}} \quad (5)$$

where

$R_{ms\ air}$ = thermal resistance of meter-side air film, $(m^2 \cdot K)/W$ $(h \cdot ft^2 \cdot °F/Btu)$
$R_{cs\ air}$ = thermal resistance of climate-side air film, $(m^2 \cdot K)/W$ $(h \cdot ft^2 \cdot °F/Btu)$
A_{wall} = area of wall, m^2 (ft^2)
T_{ms} = average meter-side surface temperature, °C (°F)
T_{ma} = average meter-side air temperature, °C (°F)
T_{cs} = average climate-side surface temperature, °C (°F)
T_{ca} = average climate-side air temperature, °C (°F)

The overall air-to-air thermal resistance of the wall assembly $R_{u\ wall}$ is calculated from

$$R_{u\ wall} = \frac{A_{wall} \cdot (T_{ma} - T_{ca})}{Q_{wall}} \quad (6)$$

or

$$R_{u\ wall} = R_{wall} + R_{ms\ air} + R_{cs\ air} \quad (7)$$

where

$R_{u\ wall}$ = overall air-to-air thermal resistance of wall assembly, $(m^2 \cdot K)/W$ $(h \cdot ft^2 \cdot °F/Btu)$
A_{wall} = area of wall, m^2 (ft^2)
T_{ma} = average metering-side air temperature, °C (°F)
T_{ca} = average climate-side air temperature, °C (°F)
$R_{ms\ air}$ = thermal resistance of meter-side air film, $(m^2 \cdot K)/W$ $(h \cdot ft^2 \cdot °F/Btu)$
$R_{cs\ air}$ = thermal resistance of climate-side air film, $(m^2 \cdot K)/W$ $(h \cdot ft^2 \cdot °F/Btu)$

Table 1 summarizes the calculated wall systems' heat flows and R-values as well as the temperature data needed for those calculations. The temperatures and heat flows presented for tests 1 and 2 are averages for the time interval for the test after steady state had been achieved. When multiple thermocouples are used to define a temperature, the collection of sensors is averaged for each scan and then integrated over the time interval. Surface-to-surface R-values are shown in bold. Corresponding values of the temperatures, heat flow rates, and R-values in SI units are provided before their U.S. unit system equivalents in parentheses. In later sections, only the U.S. unit system values are used.

There is an R-6 or 73% increase in the steady-state thermal resistance of the 2 × 4 steel stud wall by adding the stud-snuggler and using thicker fiberglass batts. As per the *ASTM Standard C1363* procedure, the measurement accuracy is about 8% to 10%.

THEORETICAL CALCULATIONS

Numerical simulations were done using a finite-difference model, Heating 7.2 (Childs 1993), to evaluate the steady-state thermal performance of wood and steel stud wall assemblies. Effects of adding the stud-snugglers as well as different framing factors were investigated. Framing factor refers to the percentage of the wall area occupied by the wood or steel studs. Five wall assemblies with different frame types were simulated: (1) 2 × 6 wood studs, (2) 2 × 4 wood studs with stud-snugglers (SS 2 × 4 wood), (3) 2 × 4 steel studs with stud-snugglers (SS 2 × 4 steel), (4) 2 × 4 steel studs, and (5) 2 × 6 steel studs. Different combinations of insulation and framing factor were used in the simulations for the same boundary conditions as during the hot-box testing. For each assembly, thermal

Table 1. Hot-box Test Results for 2 × 4 Steel-Framed Wall Assemblies with Studs Installed at 24 in. on Center

	Test 1: Stud-Snuggler (R-19 Insulation)	Test 2: Conventional 2 × 4 Studs (R-13 Insulation)
T_{cs}, °C (°F)	9.72 (49.5)	9.56 (49.2)
T_{ms}, °C (°F)	37.78 (100.0)	37.78 (100.0)
T_{ma}, °C (°F)	38.94 (102.1)	39.78 (103.6)
T_{ca}, °C (°F)	9.11 (48.4)	8.50 (47.3)
?T, °C (°F)	10.28 (50.5)	10.44 (50.8)
T(mean), °C (°F)	23.72 (74.7)	23.67 (74.6)
$Q_{mb,\,fl}$, W (Btu/h)	(4.850)	(16.358)
Q_{wall}, W (Btu/h)	66.92 (228.35)	116.82 (398.61)
R_{wall}, (m²·K)/W (h·ft²·°F/Btu)	**2.50 (14.2)**	**1.44 (8.2)**
$R_{u,\,wall}$, (m²·K)/W (h·ft²·°F/Btu)	2.64 (15.0)	1.59 (9.0)
$R_{ms,\,air}$, (m²·K)/W (h·ft²·°F/Btu)	0.103 (0.584)	0.101 (0.571)
$R_{cs,\,air}$, (m²·K)/W (h·ft²·°F/Btu)	0.052 (0.298)	0.055 (0.313)

performance was evaluated numerically for fiberglass batts with framing factors of 6%, 10%, and 15%. Batts 9 cm (3.5 in.) thick were used in the simulation of the 2 × 4 steel stud wall, and 14 cm (5.5 in.) thick batts were used in all other simulations. Further, simulations were done using the properties of blown fiberglass insulation (Johns Manville Spider [no date]) along with 6% framing factor. Thermal resistivities of the fiberglass batt and blown fiberglass insulation used in thermal modeling were R-23.9 (m·K)/W (R-3.45 h·ft²·°F/Btu/in.) and R-28.5 (m·K)/W (R-4.11 h·ft²·°F/Btu/in.), respectively.

The resulting R-values for each wall frame type and insulation-framing factor combination are shown in Figure 6. While comparing conventional 2 × 4 construction with the 2 × 4 and stud-snuggler construction, the increase in steady-state R-value is expected due to the application of thicker insulation batts. Comparison of 2 × 6 stud construction with the 2 × 4 construction with stud-snugglers is a better evaluation criterion for the thermal performance enhancement afforded by the introduction of the stud-snugglers. As seen in Figure 6, 2 × 4 steel construction with stud-snugglers in place (SS 2 × 4 steel) performs much better than both conventional 2 × 6 and 2 × 4 steel stud assemblies. Depending on the type of insulation and framing factors, the simulations predict improvements of 60% to 100% over the 2 × 6 assembly and 110% to 160% over the 2 × 4 assembly with steed studs. With wood studs, the improvement in the steady-state R-value is comparatively minor: the estimated increases in the R-values are 9% or less for the different wood-framed assemblies.

Comparing the calculations to the experiments, R-2.7 (m²·K)/W (R-15.35 h·ft²·°F/Btu) of the SS 2 × 4 steel configuration, with 10% framing factor, is within 10% of the measured value of R-2.5 (m²·K)/W (R-14.2 h·ft²·°F/Btu). The framing factor in the tested assembly was about 11%, which could partially explain the difference between the tested and calculated R-values.

Figure 7 shows the effects of increasing framing factors on the thermal resistance of the different wall assemblies. The different trends were obtained through regression analysis of the simulation results presented earlier. Wood stud walls clearly show superior thermal performance than steel studs. The thermal resistance of wood stud walls has an inverse and linear response to the change in framing factor. The steel-framed walls, conversely, have a nonlinear response, but also show lower resistances with higher framing factor. Application of the stud-snugglers (SS 2 × 4 steel) both increases the thermal resistance of the steel-framed walls and also makes the response to changing framing factor linear.

Figures 8 and 9 show the temperature distributions on the interior surface of steel stud walls filled with blown fiberglass insulation. In the wall represented in Figure 9, the steel studs are covered with the stud-snugglers. The imposed boundary conditions in the simulations were –6.67°C (20°F) exterior temperature and 21.1°C (70°F) interior temperature. A framing factor of 6.2% was used for both simulations. The center location of both distributions corresponds with the location of the studs, and the extremities correspond to the insulation-filled cavity.

In Figure 8, the center temperature is about 5.0°C (9°F) lower than the extremities, clearly showing signs of thermal bridging. The temperature difference is less than 1.1°C (2°F) in Figure 9, thus showing that the stud-snugglers can reduce thermal bridging. An added benefit of the stud-snugglers is elimination of "ghosting" caused by the relatively lower local temperatures. Ghosting is the discoloration of walls at the studs from accumulation of dust and possible mildew growth from moisture condensation. This problem will be more severe with conventional steel studs.

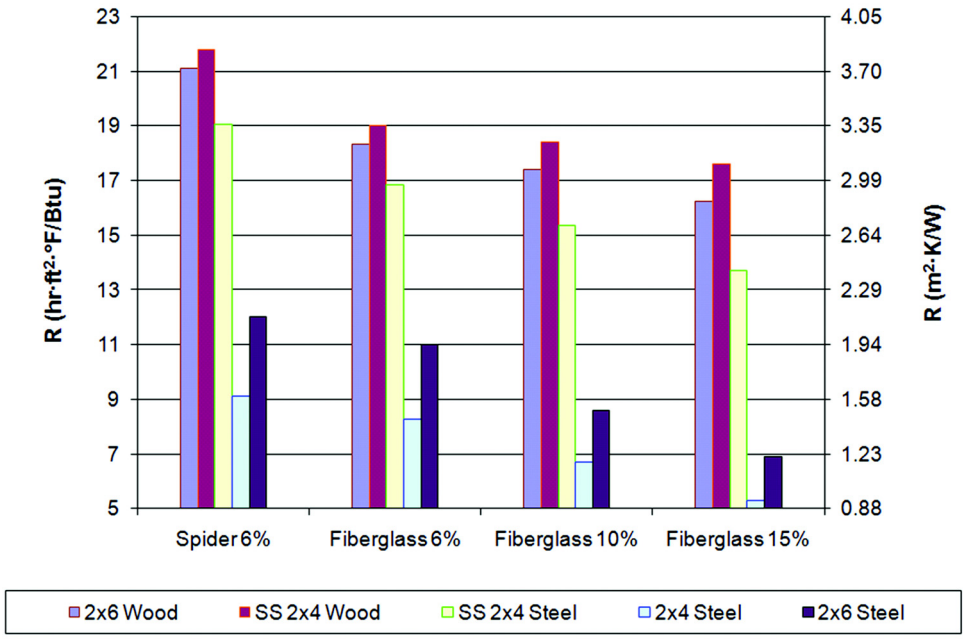

Figure 6 *Steady-state R-values of wall assemblies with different frame types and different framing factors. "SS 2 × 4" refers to studs incorporating stud-snugglers.*

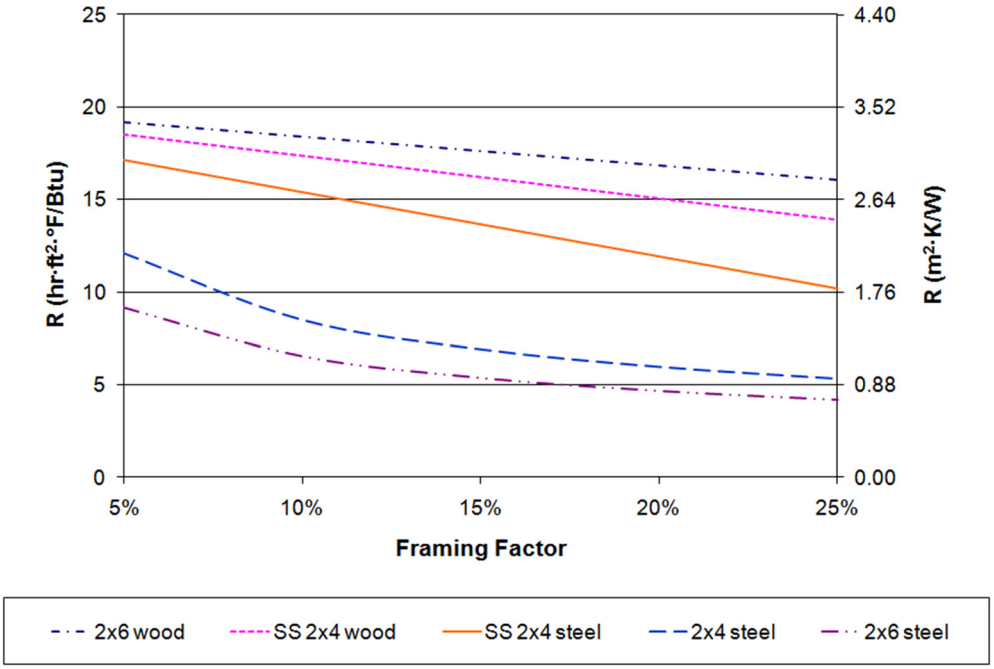

Figure 7 *Effect of framing factor on steady-state R-values of different wall assemblies with fiberglass batt insulation. "SS 2 × 4" refers to studs incorporating stud-snugglers.*

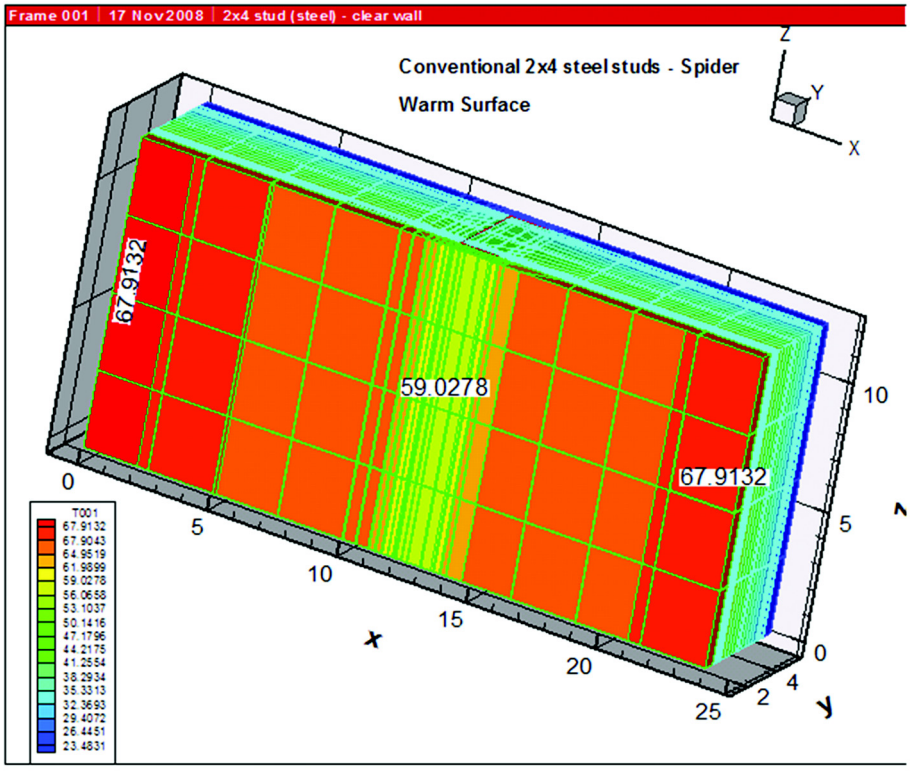

Figure 8 *Surface temperature distribution of 2 × 4 steel stud-framed wall with blown fiberglass insulation.*

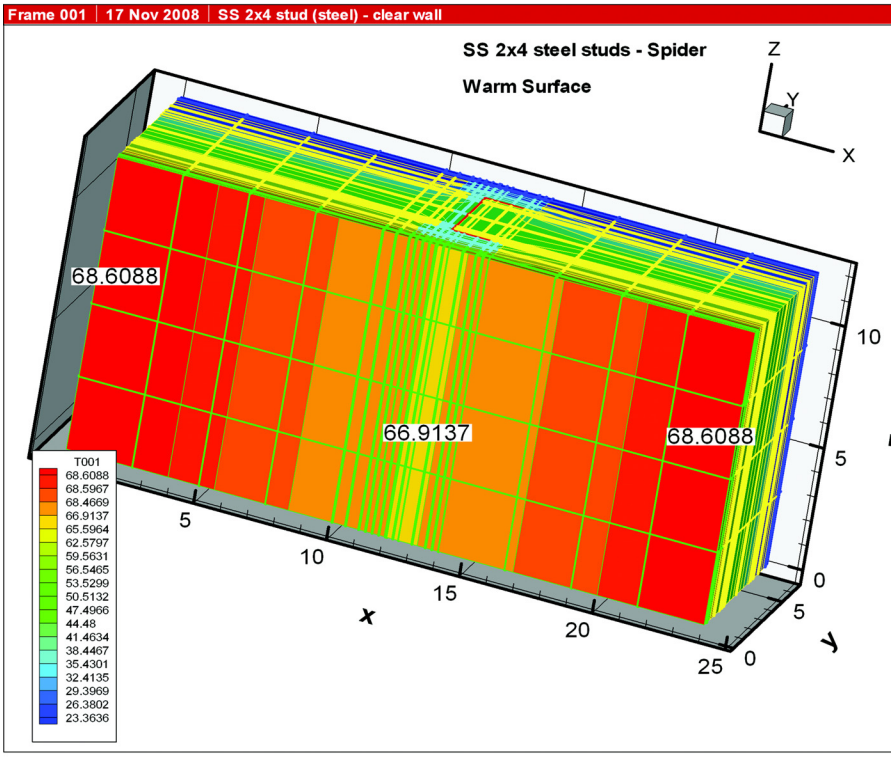

Figure 9 *Surface temperature distribution of 2 × 4 steel stud-framed wall with stud-snugglers and blown fiberglass insulation.*

SUMMARY AND CONCLUSIONS

Two configurations of steel-framed walls constructed with conventional 2 × 4 steel studs and insulated with R-19 (14 cm [5.5 in.] thick) and R-13 (9 cm [3.5 in.] thick) fiberglass insulation batts were tested in the Oak Ridge National Laboratory (ORNL) guarded hot-box using *ASTM Standard C1363*. The first test wall used conventional 2 × 4 steel studs insulated with 2.54 cm (1 in.) thick foam profiles. These foam profiles converted the 2 × 4 assembly into a 2 × 6 assembly and corresponding cavity thickness, allowing application of R-19 fiberglass insulation. The second wall tested for comparison was a conventional 2 × 4 wall using R-13 insulation batts. In both walls, the 2 × 4 steel studs were installed at 61 cm (24 in.) on center.

For the wall installed with the stud-snuggler foam profiles and R-19 (14 cm [5.5 in.] thick) fiberglass insulation, the measured surface-to-surface R-value was R-2.5 (m^2·K)/W (R-14.2 h·ft^2·°F/Btu). For the conventional 2 × 4 steel stud wall insulated with R-13 (9 cm [3.5 in.] thick) fiberglass insulation, surface-to-surface R-value was R-1.44 (m^2·K)/W (R-8.2 h·ft^2·°F/Btu). The R-value difference associated with increased thickness of the wall and application of stud-snuggler profiles was R-1.06 (m^2·K)/W (R-6 h·ft^2·°F/Btu). This is approximately a 73% improvement in thermal performance.

Numerical simulations of wood and steel stud walls, with and without the stud-snugglers, were done. The results further corroborated the substantial improvement in steady-state thermal resistance of steel frame walls incorporating the stud-snugglers, compared to both conventional 2 × 4 and 2 × 6 steel stud walls. The improvement in wood stud wall thermal resistance due to the addition of the stud-snugglers was relatively small. The simulations showed that addition of the stud-snugglers reduces thermal bridging in steel frame walls and can also potentially eliminate the problem of ghosting.

NOMENCLATURE

A_{mb} = surface area of metering box, m^2 (ft^2)

A_{wall} = area of wall, m^2 (ft^2)

Q_{fan} = energy input to fans in metering chamber, W (Btu/h)

Q_h = energy input to resistance heaters in metering chamber, W (Btu/h)

Q_{mb} = energy exchange through meter box walls, W (Btu/h)

Q_{TOTAL} = total energy exchange through test wall, W (Btu/h)

Q_{wall} = total energy flow through wall assembly from metering to climate chamber, W (Btu/h)

$R_{cs\ air}$ = climate-side air film thermal resistance, (m^2·K)/W (h·ft^2·°F/Btu)

R_{mb} = thermal resistance of the metering box walls, (m^2·K)/W (h·ft^2·°F/Btu)

$R_{ms\ air}$ = meter-side air film thermal resistance, (m^2·K)/W (h·ft^2·°F/Btu)

$R_{u\ wall}$ = overall R-value of sample wall, $R_{ms\ air} + R_{wall} + R_{cs\ air}$, ($m^2$·K)/W (h·$ft^2$·°F/Btu)

R_{wall} = surface-to-surface thermal resistance of wall assembly, (m^2·K)/W (h·ft^2·°F/Btu)

$R_{wall\ ext}$ = surface-to-surface R-value of wall, (m^2·K)/W (h·ft^2·°F/Btu)

T_{ca} = average of 48 air thermocouples (TCs), climate side, °C (°F)

T_{cs} = weighted average climate-side external surface temperature, °C (°F)

T_{ma} = average of 36 air TCs, meter side, °C (°F)

T_{mb} = temperature imbalance across metering box walls, °C (°F)

T(mean) = average weighted exterior wall surface mean temperature, °C (°F)

T_{ms} = weighted average meter-side external surface temperature, °C (°F)

ΔT_{EXT} = average weighted exterior wall surface temperature difference, °C (°F)

REFERENCES

ASTM. 2009. *ASTM Standard C645-09a, Standard Specification for Nonstructural Steel Framing Members*. West Conshohocken, PA: American Society for Testing and Materials.

ASTM. 1997. *ASTM Standard C1363-97, Standard Test Method for Thermal Performance of Building Materials by Means of a Hot Box Apparatus*, v. 04.06. West Conshohocken, PA: American Society for Testing and Materials.

Childs, K.W. 1993. *Heating 7.2 user's manual*. Report ORNL/TM-12262. Oak Ridge, TN: Oak Ridge National Laboratory.

Johns Manville Spider® Custom Insulation. (no date). *JM Spider® custom insulation system data sheet*. http://www.specjm.com/products/sprayin2/spider.asp.

Kosny, J., J.E. Christian, and A.O. Desjarlais. 1997. Thermal breaking systems for metal stud walls—Can metal stud walls perform as well as wood stud walls? *ASHRAE Transactions* 103(1).

Kosny, J., P.W. Childs, and M. Gorgolewski. 2002. New developments from ORNL: A new generation of steel framing technologies. *World Sustainable Steel Congress*, Luxemburg.

Kossecka, E., Kosny, J., 2008, - "Hot-Box Testing of Building Envelope Assemblies - A Simplified Procedure for Estimation of Minimum Time of the Test", Journal of Testing and Evaluation, Vol. 36, No. 3, p 242-249.

Kosny, J. and P.W. Childs. 2002. *Accuracy of hot box testing of steel stud walls insulation materials: Testing and applications*, vol. 4. ASTM STP 1426, A.O. Desjarlais,

and R.R. Zarr, eds. West Conshohocken, PA: American Society for Testing and Materials.